Mixed Reality Interface for Whole-Body Balancing and Manipulation of Humanoid Robot

Hyunjong Song, Gabriel Bronfman, Yunxiang Zhang, Qi Sun, and Joo H. Kim, *Senior Member IEEE*

***Abstract*— Although there have been considerable advancements in the field of humanoid robotics, the widespread utilization of humanoid robots remains a distant goal. One roadblock is the complexity of the control and operating software. In this work, we introduce a novel approach to humanoid robot control by leveraging a mixed reality (MR) interface for whole-body balancing and manipulation. This interface system uses an MR headset to track the operator's movement and provide the operator with useful visual information for the control. The robot mimics the operator's movement through a motion retargeting method based on linear scaling and inverse kinematics. The operator obtains visual access to the robot's perspective view augmented with fiducial detection and monitors the current stability of the robot by comparing the precomputed balanced state basin and the robot's center-of-mass state in real-time. In real experiments, the operator successfully controlled the robot to grasp and lift an object without falling. The common issues in teleoperation with virtual reality headsets, motion sickness and unawareness of their surroundings, are reduced to a low level. This work demonstrates the potential of MR in teleoperation with a motion retargeting and stability monitoring method.**

I. Introduction

Despite recent advancements in the field of humanoid robotics, the widespread utilization of humanoid robots remains a distant goal. One reason is the complexity of the control and operating software. As a potential solution to this challenge, teleoperation has become a growing source of interest in the robotics community because it can merge the human-dominated realm of cognition with the robot-dominated realm of physical capability. The state-of-the-art and growing interests in this field were notably showcased in the $10M ANA Avatar XPRIZE competition in 2022 [1]–[6].

According to a recent survey on teleoperation in robotics [7] and insights from the competition, there exists a need for an immersive and intuitive interface for operators that accommodates the complexity of humanoid robot control. Consequently, researchers have explored virtual reality (VR) devices for remote whole-body control of robots with motion retargeting [7]–[10]. VR offers more awareness of the robot's task space than the traditional control interface for operators, and motion retargeting enables the robot to mimic the operator's physical movements. This advantage has demonstrated that a relatively inexperienced operator can more easily achieve complex tasks [7]–[9]. However, there are limitations to using VR devices. Operators can suffer from motion sickness due to VR-induced visual discrepancies and unawareness of their surroundings [7], [11].

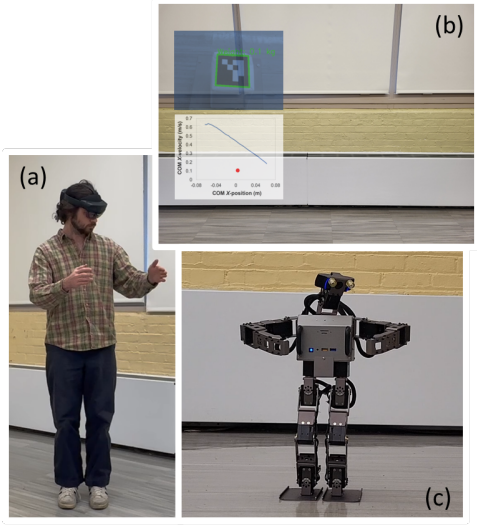

Figure 1. The proposed teleoperation interface (a) Operator wearing HoloLens headset (b) Composite image of the operator's view. On top is an augmented robot view with the detected tags' location and weight within the view. On the bottom is displaying the robot's balancing status at the current moment. (c) OP3 imitating the behavior of the operator

One promising avenue for addressing these limitations is the integration of mixed reality (MR) devices into teleoperation interfaces [12]. Unlike VR devices, MR devices have a transparent visor or glasses onto which virtual objects are projected. This feature not only reduces the risk of motion sickness by providing local situational awareness, but also creates an immersive experience through real-time coexistence and interaction between physical and digital entities. This is a major advancement over VR wherein the operator can achieve tasks in the teleoperation space while overcoming its limitations.

However, there exist vast physical differences between human operators and humanoid robots, such as link/limb lengths, mass properties, degrees of freedom (DOF), and actuation limits. Thus, their stability during a task can significantly differ even if they take a similar pose. The balance stability of the robot cannot be perceived or controlled directly by the operator. For successful task fulfillment, the robots' balance stability must be accurately evaluated and intuitively recognizable for the operators to immediately take proper action when needed. Furthermore, considering the context of

*Research supported in part by the Center for Urban Science and Progress (CUSP) at New York University.

H. Song, G. Bronfman, and J. H. Kim are with the Department of Mechanical and Aerospace Engineering at New York University, Brooklyn, NY 11201 USA (e-mail: joo.h.kim@nyu.edu).

Y. Zhang and Q. Sun are with CUSP and the Department of Computer Science and Engineering at New York University, Brooklyn, NY 11201 USA.

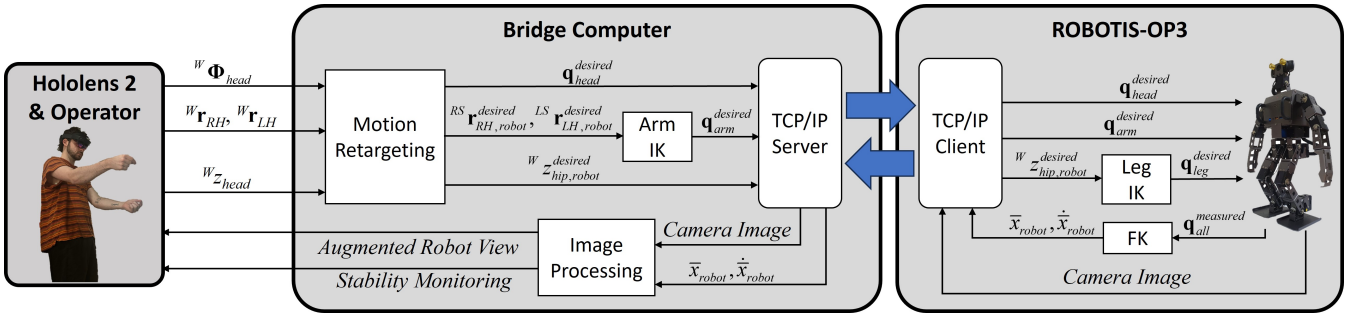

Figure 2. Architecture diagram for system. Black arrows indicate communication between components of software, while blue arrows indicate true TCP/IP connections. Constant feedback between robot, the windows PC, and the HoloLens is occurring to ensure operator commands are communicated and the state of OP3 is being accurately relayed.

teleoperation involving loco-manipulation tasks, such as lifting, the evaluation must involve whole-body dynamics and system-specific properties and capabilities. In prior works [13]–[17], optimization-based frameworks have been established to construct accurate balance criteria for the identification of the system's stability state under various conditions such as standing, walking, and lifting. The balance criteria are the balanced state basins (BSBs) that are partitions within the center-of-mass- (COM) state space augmented with kinematic and actuation limits, full-order dynamics with a whole-body model, task requirements, and balanced state definition. It is validated that the BSBs can accurately quantify the balancing capability of the system [13]–[16] and identify unbalanced states right after a perturbation [17]. In this regard, the BSBs can be used to provide the operators with accurate and intuitive information on the current stability of the robot.

In this work, a preliminary interface to control a humanoid robot using an MR headset is developed (Fig. 1). This approach is a user-in-the-loop method that enables puppeteering wherein the robot mimics the operator's physical movements without the use of any controllers. The target positions of the robot's hands and hip are found by linearly scaled positions of the analogous part of the operator, and the joint angles of the robot are computed through inverse kinematics (IK) of arms and legs. Fiducial detection is used to display information about the objects in the robot's environment to the operator. The operator can maintain the stability of the robot throughout a grasping and lifting object task by monitoring the comparison with the precomputed BSBs and the COM state of the robot. The transparent nature of the headset addresses common issues, such as the operators' motion sickness and unawareness of their surroundings, encountered in VR-based approaches. Removing the controllers enhances intuitiveness, and synchronicity of human-robot interaction, to make the given tasks more natural and efficient. This allows the overall interface system to be more lightweight without the need for adaptation to a controller. This advancement represents a significant step forward in the field of teleoperation, leveraging the potential of MR to overcome the challenges of traditional teleoperation methods for humanoid robots' loco-manipulation tasks [6].

II. Robot Platform and MR Equipment

The proposed interface is comprised of a HoloLens 2 MR headset (Microsoft Co., Ltd, USA), a bridge computer, a ROBOTIS-OP3 humanoid robot (ROBOTIS Co., Ltd, South Korea), and a router (Fig. 2). All devices are connected to the router, thereby placing them within the same network. However, no direct connection between the headset and the robot is implemented to reflect the typical teleoperation scenario where a considerable distance separates the operator and the robot. The headset has transparent glasses that project visuals into the operator's view without completely obstructing the outside world. The headset is equipped with built-in cameras for hand tracking and an inertial measurement unit for estimating the position and orientation of the head. The robot is a platform for humanoid robotics research. It has a height of 0.51 m, a weight of 3.5 kg, 20 servomotors (2 for head, 3 for each arm, 6 for each leg), a camera, a sensor board with a 3-axis gyroscope and accelerometer, and a single-board computer.

III. MR Interface System Architecture

The architecture of the proposed interface system includes the devices, software elements, and exchanged data among them (Fig. 2). The headset and the robot can only exchange data through the bridge computer, to which they are wirelessly connected. The connection between the computer and the robot is established using the Transmission Control Protocol/Internet Protocol (TCP/IP).

The robot sends the image from the camera mounted on its head and its COM state ($\bar{x}_{robot}$ and $\dot{\bar{x}}_{robot}$, where $\bar{x}_{robot}$ is the COM X-position of the robot and the dot represents time-derivative) estimated by forward kinematics (FK) using the measured angles of all joints $\mathbf{q}_{all}^{measured}$ to the bridge computer. The camera image is used to generate the augmented robot view by detecting ArUco tags attached to the object in the task space of the robot and then displaying the weight of the object over the detected tags. A stability monitoring image is created by overlaying $\bar{x}_{robot}$ and $\dot{\bar{x}}_{robot}$ on the precomputed BSB in the COM state space. Both the augmented robot view and the stability monitoring image are transmitted to the headset and then shown in two separate floating windows for the operator (Fig. 1 (b)).

The headset tracks the operator's right-hand position vector ${}^{W}\mathbf{r}_{RH}$, left-hand position vector ${}^{W}\mathbf{r}_{LH}$, head orientation vector ${}^{W}\mathbf{\Phi}_{head}$, and head height ${}^{W}z_{head}$ with respect to the world frame W. These values are retargeted to determine the

joint angles of the robot, considering the disparity in DOFs and joint structures between the operator and the robot. This motion retargeting is achieved through linear scaling and the IK of the arms and legs. The arm IK is computed by the bridge computer while the leg IK is computed by the robot.

IV. Human-to-Robot Motion Retargeting Method

For the realism of the teleoperation, the desired head joint angles of the robot $\mathbf{q}_{head}^{desired}$ are determined by incorporating the pitch and yaw angles obtained from ${}^{W}\mathbf{\Phi}_{head}$. This ensures that the robot and the operator share a common environmental view angle.

Since the robot and the operator have different physical dimensions, a motion retargeting method is needed to translate the operator's poses into the task space of the robot. In this work, an existing simple linear scaling method [18] is used. The scaling factor for the arm λ_{arm} is determined as follows:

$$\lambda_{arm} = \frac{l_{arm,robot}}{l_{arm,operator}} \tag{1}$$

where $l_{arm,\,robot}$ and $l_{arm,\,operator}$ are the lengths of the robot's and the operator's arm, respectively. The robot's desired right-hand position vector with respect to the right shoulder ${}^{RS}\mathbf{r}_{RH,robot}^{desired}$ and desired left-hand position vector with respect to the left shoulder ${}^{LS}\mathbf{r}_{LH,robot}^{desired}$ are decided by the following equations:

$${}^{RS}\mathbf{r}_{RH,robot}^{desired} = \lambda_{arm}\,{}^{RS}\mathbf{r}_{RH} = \lambda_{arm}({}^{W}\mathbf{r}_{RH} - {}^{W}\mathbf{r}_{RS}) \tag{2}$$

$${}^{LS}\mathbf{r}_{LH,robot}^{desired} = \lambda_{arm}\,{}^{LS}\mathbf{r}_{LH} = \lambda_{arm}({}^{W}\mathbf{r}_{LH} - {}^{W}\mathbf{r}_{LS}) \tag{3}$$

where ${}^{RS}\mathbf{r}_{RH}$ and ${}^{LS}\mathbf{r}_{LH}$ are the position vectors of the operator's right hand and left hand with respect to their right and left shoulder, respectively; ${}^{W}\mathbf{r}_{RS}$ and ${}^{W}\mathbf{r}_{LS}$ are the position vectors of the operator's right and left shoulder with respect to W, respectively. The robot's desired arm joint angles $\mathbf{q}_{arm}^{desired}$ are computed with the arm IK using ${}^{RS}\mathbf{r}_{RH,\,robot}$ and ${}^{LS}\mathbf{r}_{LH,\,robot}$.

A similar method is employed for the leg motion. The scaling factor for the leg λ_{leg} is determined as follows:

$$\lambda_{leg} = \frac{h_{hip,operator}}{h_{head,operator}} \cdot \frac{h_{hip,robot}}{h_{hip,operator}} = \frac{h_{hip,robot}}{h_{head,operator}} \tag{4}$$

where $h_{head,\,operator}$ is the head height of the operator; $h_{hip,\,operator}$ is the hip height of the operator; $h_{hip,\,robot}$ is the hip height of the robot. All these heights are measured in a standing straight position. The desired hip height of the robot ${}^{W}z_{hip,robot}^{desired}$ is determined by the following equation:

$${}^{W}z_{hip,robot}^{desired} = \lambda_{leg}\,{}^{W}z_{head} \tag{5}$$

The robot's desired leg joint angles $\mathbf{q}_{leg}^{desired}$ are computed with the leg IK using ${}^{W}z_{hip,robot}^{desired}$. The robot's hip orientation is set to be parallel to the ground and both feet maintain the zero step length and full contact with even ground.

V. Balanced State Basin Construction

The BSB is formed by the balanced state boundaries which are computed by the optimization-based framework from prior work [13]–[17]. The balanced state boundaries for the grasping and lifting object task in the robot's COM-state space are constructed by the set of solutions of a series of optimization problems that maximize the initial COM X-velocity of the robot $\dot{\bar{x}}_{robot}(0)$ in both forward and backward directions at each sampled whole-body pose. The optimization problems are subject to the system- and task-specific constraints and the solutions are the pairs of the $\bar{x}_{robot}$ of each sampled whole-body pose and the maximized $\dot{\bar{x}}_{robot}(0)$. The sagittal plane is chosen as the plane of interest. The formulation of the problem is as follows:

$$\max_{\mathbf{v},\boldsymbol{\alpha}} \dot{\bar{x}}_{robot}(0) \text{ subject to } \mathbf{b}^{LB} \le \mathbf{b}(\mathbf{v},\boldsymbol{\alpha}) \le \mathbf{b}^{UB} \tag{6}$$

where $\mathbf{b}$ is the vector of constraint functions and the superscripts LB and UB are the lower and upper bounds of the constraint functions, respectively. The constraint functions vector $\mathbf{b}$ reflects system-specific properties such as kinematic and actuation limits and general constraints related to contact interactions (unilateral normal contact force, friction cone, COP bounds, foot configuration, and the non-existence of undesired contacts). The constraints are imposed during the solution time interval [0, T], where T is the terminal time.

The vector $\mathbf{b}$ also has task-specific constraints that represent the grasping and lifting object task requirements and the definition of the balanced state [15], [16] (no required change in contact to achieve a final static equilibrium). For the task, the identical left and right arm joint angle constraint is imposed at all times ($\forall t \in [0,T]$) to maintain holding the object:

$$\mathbf{q}_{l,arm}(t) = \mathbf{q}_{r,arm}(t) \tag{7}$$

where $\mathbf{q}_{l,arm}$ and $\mathbf{q}_{r,arm}$ denote the left and right arm joint angles, respectively. To avoid self-collision, the orientation of the object is restricted within a certain range throughout the solution time interval ($\forall t \in [0,T]$):

$$-\pi/4 \le \Phi_{object}(t) \le \pi/2 \tag{8}$$

where Φ_{object} is the orientation of the object. As initial conditions, the sampled whole-body poses are imposed:

$$\mathbf{q}_{all}(0) = \mathbf{q}_{all}^{sampled} \tag{9}$$

For the definition of the balanced state, a COM static equilibrium at the desired COM X-position is imposed as a final condition:

$$\bar{x}_{robot}(T) = \bar{x}_{robot}^{desired} \tag{10}$$

$$\dot{\bar{x}}_{robot}(T) = \ddot{\bar{x}}_{robot}(T) = \dot{\bar{z}}_{robot}(T) = \ddot{\bar{z}}_{robot}(T) = 0 \tag{11}$$

where $\bar{z}_{robot}$ is the COM Z-position of the robot. In addition, both feet are fixed with zero step length at all times ($\forall t \in [0,T]$):

$${}^{W}\mathbf{r}_{l,foot}(t) = {}^{W}\mathbf{r}_{r,foot}(t) = \mathbf{0};\ \Phi_{lfoot}(t) = \Phi_{rfoot}(t) = 0 \tag{12}$$

where ${}^{W}\mathbf{r}_{l,foot}$, ${}^{W}\mathbf{r}_{r,foot}$, Φ_{lfoot}, and Φ_{rfoot} are the position vectors of the left and right foot and the orientation of the left and right foot, respectively.

VI. Results and Discussion

The proposed MR interface system was implemented and tested in a real experiment (Fig. 3). With the proposed MR interface system, the operator successfully controlled the robot to conduct the grasping and lifting object task without any falls on the first use of the system although the operator was not able to see the robot and had to only depend on the interface during the task. This minimal adaptation time shows the interface provides an effective control method

The operator could understand the task space of the robot by watching the augmented robot view and the robot's balancing status through the stability monitoring image. The operator can gauge the stability margin by comparing the current COM state of the robot and the BSB (Fig. 4). This stability monitoring approach can enable a user-in-the-loop to ensure that overall situational awareness is enhanced. The balanced state boundaries for forward and backward directions were computed at whole-body poses sampled from their COM *X*-positions within the base of support and constructed the BSB (Fig. 4). Due to the negligible weight of the object, it was not considered when constructing the BSB.

The BSB was validated by tests in the Webots simulation environment (Cyberbotics Ltd., Switzerland). Force perturbations were used for the robot to have the COM states inside and outside of the BSB. The robot utilized the hip strategy from prior works [15], [19] to maintain balance (Fig. 5). The COM state trajectory initiated inside the BSB stayed within and the trajectory originating outside remained outside with an eventual falling (Fig. 4 and 5). This confirms the validity of the BSB as a balance criterion.

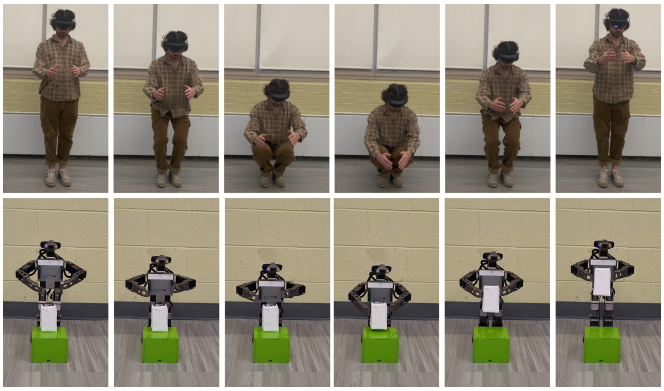

Figure 3. Experiment snapshots of the operator (top) and the robot (bottom).

The operator also could recognize the limited hand tracking range of the headset through the display of red spheres on each palm, which indicates whether the hand is being tracked. This enabled the operator to determine the optimal hand placement for task fulfillment. During the experiment, the transparent nature of the headset allowed the operator to maintain a clear view of the real world. This reduced the risk of motion sickness induced by a jittery or inconsistent virtual environment.

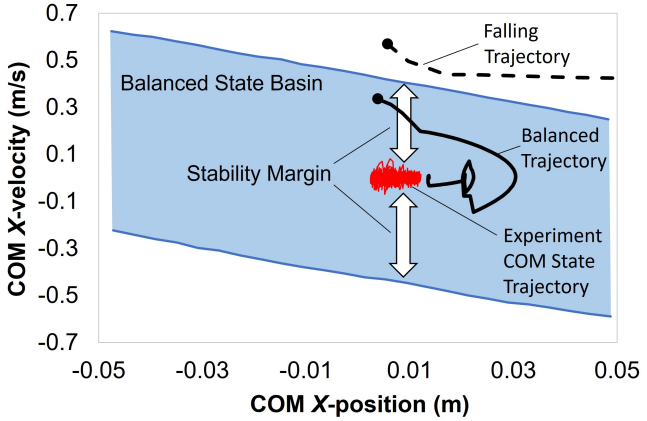

Figure 4. The precomputed BSB (blue shaded), balanced (black solid) and falling (black dashed) COM state trajectories from the simulation, and experiment COM state trajectory (red) that was recorded during the task. The stability margin is the gap between the current and the maximized COM *X*-velocities in the forward and backward directions at the COM *X*-position.

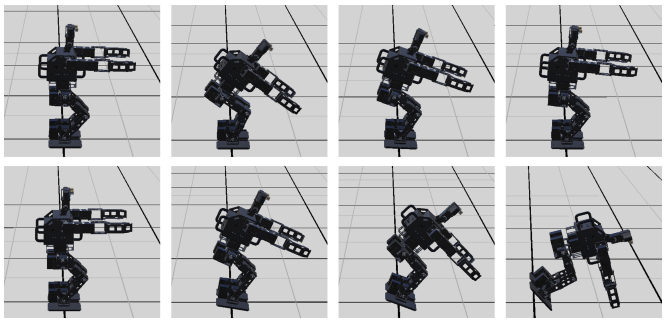

Figure 5. The snapshots of the simulation tests for the validation of the BSB. The robot maintains balance from the initial perturbed state within the BSB (top), while falling down from the state outside the BSB (bottom).

The default setting of the servomotor of the robot was used except for the profile acceleration [20] which automatically enables a trapezoidal velocity profile. Due to the 45 Hz hand tracking frequency of the headset, which is considered slow for robot control and can make the input motion jerky, the profile acceleration was set to the lowest value for the smooth motion of the robot. From the recorded desired and measured joint angles and hip height (Fig. 6) trajectories, this profile acceleration setting effectively removes noise in the desired values and results in the smoother robot motion compared to the given input motion. However, some delays are also observed in the trajectories due to the decreased bandwidth of the servomotors induced by the setting. This required the operator to keep the movement deliberately slow.

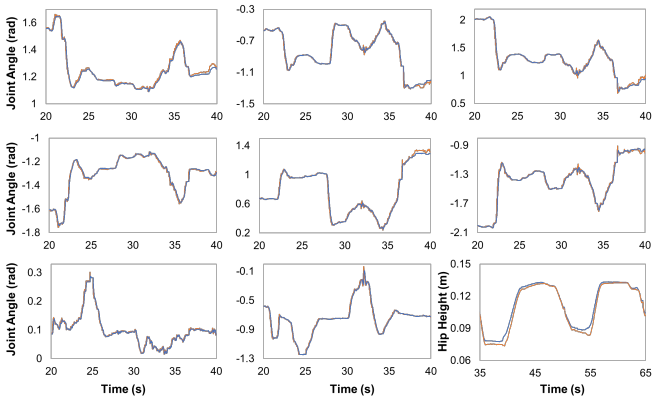

Figure 6. Desired and measured values during the operator's random motion. Desired values are represented by the blue curves, while the orange curves denote the measured values. The right shoulder pitch (top left), right shoulder roll (top middle), right elbow (top right), left shoulder pitch (middle left), left shoulder roll (middle), left elbow (middle right), head pan (bottom left), head tilt (bottom middle), and hip height (bottom right) are shown.

VII. Conclusion

This research presents an innovative approach to humanoid robot teleoperation, leveraging mixed reality (MR) technology to enhance human-robot interaction. Utilizing the HoloLens 2 MR headset allows the operator to control the ROBOTIS-OP3 humanoid robot to mimic the operator's natural body movements without the use of any additional controllers. This setup is comprised of a bridge computer processing communication and visual inputs from the robot and projecting them onto the headset display.

The current work can be extended for more complex loco-manipulation tasks by including hand-gesture-based communication and voice recognition to command the diverse actions of the robots such as walking and turning. This would provide more insight into MR as a control interface.

More MR-based feedback for the operator would increase situational awareness. Using a so-called "virtual surrogate" would enable the operator to see a virtual representation of the state of the robot they are controlling, thereby making control easier. Additional MR components could be added to enrich the task space of the operator, providing more clarifying visual feedback.

Lifting heavier objects is another task that could be explored. To enable a BSB-based, user-in-the-loop approach for heavier object lifting, information about the weight of the object would be needed to select a proper pose for the robot. Additionally, more comprehensive BSBs considering the weight of the object can be incorporated into the interface system.

References

[1] Behnke, S., Adams, J. A., and Locke, D., "The $10 Million ANA Avatar XPRIZE Competition: How It Advanced Immersive Telepresence Systems," *IEEE Robotics and Automation Magazine*, Vol. 30, n 4, pp. 98–104, December 2023.

[2] Correia Marques, J. M., Naughton, P., Peng, J.-C., Zhu, Y., Nam, J. S., Kong, Q., Zhang, X., *et al.*, "Immersive Commodity Telepresence with the AVATRINA Robot Avatar," *International Journal of Social Robotics*, January 2024.

[3] Schwarz, M., Lenz, C., Memmesheimer, R., Pätzold, B., Rochow, A., Schreiber, M., and Behnke, S., "Robust Immersive Telepresence and Mobile Telemanipulation: NimbRo wins ANA Avatar XPRIZE Finals," *IEEE-RAS 22nd International Conference on Humanoid Robots* , Decemberr 12-14, 2023, Austin, TX, USA.

[4] Sung, E., You, S., Kim, S., and Park, J., "SNU-Avatar Robot Hand: Dexterous Robot Hand with Prismatic Four-Bar Linkage for Versatile Daily Applications," *IEEE-RAS International Conference on Humanoid Robots*, December 12-14, 2023, Austin, TX, USA.

[5] Tran, T., Chagas Vaz, J., Kosanovic, N., and Oh, P., "Highly Dexterous Humanoid Manipulator (HDHM) Designed for Avatar Systems," *Digest of Technical Papers - IEEE International Conference on Consumer Electronics*, January 06-08, 2023, Las Vegas, NV, USA, Vol. 2023-January.

[6] Vaz, J. C., Kosanovic, N., and Oh, P., "ART: Avatar Robotics Telepresence—the future of humanoid material handling loco-manipulation," *Intelligent Service Robotics*, 2023.

[7] Darvish, K., Penco, L., Ramos, J., Cisneros, R., Pratt, J., Yoshida, E., Ivaldi, S., *et al.*, "Teleoperation of Humanoid Robots: A Survey," *IEEE Transactions on Robotics*, Vol. 29, n 3, pp. 1706–1727, June 2023.

[8] Vaz, J. C., Wallace, D., and Oh, P. Y., "Humanoid loco-manipulation of pushed carts utilizing virtual reality teleoperation," *ASME International Mechanical Engineering Congress and Exposition, Proceedings (IMECE)*, American Society of Mechanical Engineers (ASME), 2021, Vol. 7B-2021.

[9] Kim, D., You, B. J., and Oh, S. R., "Chapter Whole body motion control framework for arbitrarily and simultaneously assigned upper-body tasks and walking motion," in *Cognitive Systems Monographs*, Vol. 18Springer Verlag, pp. 87–98, 2013.

[10] Dafarra, S., Pattacini, U., Romualdi, G., Rapetti, L., Grieco, R., Darvish, K., Milani, G., *et al.*, "iCub3 avatar system: Enabling remote fully immersive embodiment of humanoid robots," *Science Robotics*, Vol. 9, n 86, January 2024.

[11] Chen, Y., Sun, L., Benallegue, M., Cisneros-Limon, R., Singh, R. P., Kaneko, K., Tanguy, A., *et al.*, "Enhanced Visual Feedback with Decoupled Viewpoint Control in Immersive Humanoid Robot Teleoperation using SLAM," *IEEE-RAS International Conference on Humanoid Robots*, IEEE Computer Society, 2022, Vol. 2022-November.

[12] Vovk, A., Wild, F., Guest, W., and Kuula, T., "Simulator sickness in Augmented Reality training using the Microsoft HoloLens," *Conference on*

Human Factors in Computing Systems - Proceedings, April 21-26, 2018, Montréal, QC, Canada, Vol. 2018-April.

[13] Song, H., Peng, W. Z., and Kim, J. H., "Lifting task stability evaluation based on balanced state basins of a humanoid robot," *ASME IDETC/CIE Mechanisms and Robotics Conference*, August 20–23, 2023, Boston, MA, USA.

[14] Song, H., Peng, W. Z., and Kim, J. H., "Effects of object mass on balancing for whole-body lifting tasks," *IEEE-RAS 22nd International Conference on Humanoid Robots (Humanoids)*, December 12-14, 2023, Austin, TX, USA.

[15] Peng, W. Z., Mummolo, C., Song, H., and Kim, J. H., "Whole-body balance stability regions for multi-level momentum and stepping strategies," *Mechanism and Machine Theory*, Vol. 174, p. 104880, August 2022.

[16] Peng, W. Z., Song, H., and Kim, J. H., "Stability region-based analysis of walking and push recovery control," *ASME Journal of Mechanisms and Robotics*, Vol. 13, n 3, pp. 031103/1–031103/11, June 2021.

[17] Peng, W. Z., Song, H., and Kim, J. H., "Reduced-order model with foot tipping allowance for legged balancing," *ASME International Design Engineering Technical Conferences and Computers and Information in Engineering Conference (IDETC)*, August 17-19, 2021.

[18] Rakita, D., Mutlu, B., and Gleicher, M., "A Motion Retargeting Method for Effective Mimicry-based Teleoperation of Robot Arms," *ACM/IEEE International Conference on Human-Robot Interaction*, March 6-9, 2017, Vienna, Austria, Vol. Part F127194.

[19] Song, H., Peng, W. Z., and Kim, J. H., "Partition-aware stability control for humanoid robot push recovery with whole-body capturability," *ASME Journal of Mechanisms and Robotics*, Vol. 16, n 1, January 2024.

[20] "ROBOTIS e-Manual XM430-W350-T/R." [Online]. Available: https://emanual.robotis.com/docs/en/dxl/x/xm430-w350/.